RESEARCH PROGRAM ON
Climate Change, Agriculture and Food Security

Analysis of Historical and Projected Future Climate of Mali, West African Sahel

December 2015

Sean D. Birkel and Paul A. Mayewski

Climate Change Institute | University of Maine

Analysis of Historical and Projected Future Climate of Mali, West African Sahel

Project Report

CGIAR Research Program on Climate Change,
Agriculture and Food Security (CCAFS)

Sean D. Birkel
Paul A. Mayewski

Correct citation:
Birkel S.D., and Mayewski, P.A., 2015. Analysis of Historical and Projected Future Climate of Mali, West African Sahel. Project Report. CGIAR Research Program on Climate Change, Agriculture and Food Security (CCAFS). Copenhagen, Denmark. Available online at: www.ccafs.cgiar.org

CCAFS Reports aim to disseminate interim climate change, agriculture and food security research and practices and stimulate feedback from the scientific community.

Published by the CGIAR Research Program on Climate Change, Agriculture and Food Security (CCAFS).

The CGIAR Research Program on Climate Change, Agriculture and Food Security (CCAFS) is a strategic partnership of CGIAR and Future Earth, led by the International Center for Tropical Agriculture (CIAT). The Program is carried out with funding by CGIAR Fund Donors, the Danish International Development Agency (DANIDA), Australian Government (ACIAR), Irish Aid, Environment Canada, Ministry of Foreign Affairs for the Netherlands, Swiss Agency for Development and Cooperation (SDC), Instituto de Investigação Científica Tropical (IICT), UK Aid, Government of Russia, the European Union (EU), New Zealand Ministry of Foreign Affairs and Trade, with technical support from the International Fund for Agricultural Development (IFAD).

Contact:
CCAFS Coordinating Unit - Faculty of Science, Department of Plant and Environmental Sciences, University of Copenhagen, Rolighedsvej 21, DK-1958 Frederiksberg C, Denmark. Tel: +45 35331046; Email: ccafs@cgiar.org

Abstract

The West African country of Mali experienced devastating drought from the late 1960s to the mid 1980s, followed by partial rainfall recovery that remains below pre-1960s climatology. Here, we examine the historical and projected temperature and rainfall variability across the Malian Sahel in an effort to assist future planning for food security. Particular emphasis is placed on clarifying the teleconnection between sea-surface temperatures (SST) expressed by the Atlantic Multidecadal Oscillation (AMO) and the West African monsoon (WAM). Using gridded observations and reanalysis, we show that cool/wet (1950-1967) and warm/dry (1980-1997) end-member climates over Mali correspond to warm and cool phases of the AMO, respectively, with associated atmospheric patterns consistent with negative (slow winds, shallow poleward pressure gradient) and positive (fast winds, steep poleward gradient) modes of the North Atlantic Oscillation (NAO). These opposing climate regimes (AMO-warm/NAO-negative and AMO-cool/NAO-positive) are coupled to strength of the Sahara Low and latitudinal position of the Intertropical Convergence Zone (ITCZ), thereby accounting for changes in strength of the WAM. A case is made that multi-decade North Atlantic SST variability arises naturally from volcanic forcing and resultant changes in strength and position of the westerly winds. However, greenhouse-gas warming, stratospheric ozone depletion, and Arctic sea-ice loss is likely modifying the system behavior. In an examination of CMIP5 general circulation model (GCM) output for Mali, we find that temperature and precipitation in historical simulations fail to validate against observations, and notably do not show multi-decade variability. Atmospheric circulation across the North Atlantic is furthermore anomalously strong in CMIP5 due to an unrealistically steep pressure gradient between Azores and Iceland. These shortcomings undermine the fidelity and meaning of CMIP5 future rainfall projections across the western Sahel. We conclude here that downscale studies should target reanalysis, and investigate extreme years (e.g., cool/wet or hot/dry) as future climate analogs rather than depend on CMIP5. In all from this work, we suggest five plausible future climate scenarios for 2030-2050: 1) standard CMIP5 projection of 2 °C warming with slight rainfall decline; 2) Warming > 1 °C with rainfall remaining at present norm, or increasingly slightly due to poleward displacement of the ITCZ; 3) Warming > 1 °C with diminished rainfall or drought from southward displacement of the ITCZ; 4) Warming > 1 °C with onset of severe drought arising from renewal of high volcanic activity, and subsequent development of strong NAO-positive circulation and cool-AMO sea-surface temperature distribution; 5) Abrupt climate shift in response to collapse of summer Arctic sea ice, wherein any of the scenarios above could develop within a decade.

Keywords

Climate reanalysis; general circulation models; precipitation; climate variability; Atlantic Multidecadal Oscillation (AMO); climate prediction; Mali; west Africa; greenhouse gas warming; abrupt climate change; volcanic activity; stratospheric ozone; West African Monsoon (WAM).

About the authors

Sean David Birkel is a climate and ice sheet modeller with a specialization in climate data analysis and visualization. He is the Maine State Climatologist and Research Assistant Professor at the Climate Change Institute at the University of Maine. He has been involved in field research in Antarctica, New Zealand, and in the Western U.S. He is the lead developer of the climate and weather website Climate Reanalyzer (http://cci-reanalyzer.org).
E-mail: birkel@maine.edu

Paul Andrew Mayewski is an internationally acclaimed glaciologist, climate scientist and explorer. He is the Director of the Climate Change Institute at the University of Maine and Distinguished University of Maine Professor in the School of Earth and Climate Sciences, the School of Marine Sciences, the School of Policy and International Affairs, and the School of Business. He has led more than 60 scientific expeditions throughout the Antarctic, sub-Antarctic, Arctic, Himalayas, Tibetan Plateau and the Andes, received numerous awards, appeared regularly in many media venues, led several major multi-disciplinary, multi-national climate projects, and has written ~400 scientific publications and two popular climate books.
E-mail: paul.mayewski@maine.edu

Acknowledgements

We would like to thank graduate student Jeff Auger for assistance with model output processing. We would also like to thank the University of Maine Advanced Computing Group (UM-ACG) for computational resources.

Contents

Acronyms

AMO	Atlantic Multi-decadal Oscillation
CCSM4	NCAR Community Climate System Model Version 4
CMIP5	Coupled Model Intercomparison Project 5
GHCN	Global Historical Climatology Network
GPCC	Global Precipitation Climatology Centre
IPCC-AR5	Intergovernmental Panel on Climate Change, Assessment Report 5
ITCZ	Intertropical Convergence Zone
JRA-55	55-year Japanese Reanalysis
NNRP	NCEP/NCAR Reanalysis Project
SST	Sea Surface Temperature
UDATP	University of Delaware Air Temperature and Precipitation
WAM	West African Monsoon

Introduction

Mali is a country located in the West African Sahel (Figure 1) that has seen significant environmental challenges and political unrest in recent decades. A chief concern is the reliability of rainfall necessary for present and future food production. Precipitation across the populous southern sector of Mali originates from the West African Monsoon (WAM), a shift of winds driven by seasonal variations in solar heating that usher in either moist or dry conditions. Monsoon rainfall tends to begin in March and increases until a peak in August. The WAM develops in association with the latitudinal migration of the Intertropical Convergence Zone (ITCZ), a rainbelt encircling the globe along the thermal equator. Strength of the WAM has changed over time, most notably between ~1965 and 1985 when Sahelian rainfall underwent a marked decline, resulting in severe drought across southern Mali (Cook, 1999; Sultan and Janicot, 2003; Biasutti and Giannini, 2006). Annual rainfall has recovered somewhat since the mid 1990s, but remains below the pre-1960s instrumental-era norm. Previous studies link this drought-recovery pattern to oceanic forcing, namely changes in sea-surface temperature (SST) across the Atlantic (Hoerling et al., 2006) and Indian (Giannini et al., 2003; Bader and Latif, 2003) oceans. The lack of full rainfall recovery across the western Sahel may relate to anthropogenic warming of the tropical oceans (Zeng, 2003; Giannini et al., 2008; Rodriguez-Fonseca et al., 2011). Coupled general circulation models (GCMs) poorly reproduce SST-WAM teleconnections (Rodriguez-Fonseca et al., 2011), and thus future climate prediction for Mali remains problematic.

Here, we seek new insights into Mali's climate evolution with work driven by four objectives:

1) Interpret and assess historical climate on annual, seasonal, and monthly timescales using observational data and climate reanalysis models.
2) Develop timeseries of precipitation and heating events on a daily scale throughout the reanalysis era to assess changes in water availability.
3) Interpret output from CMIP5 general circulation models (GCMs) used to project future climate with particular regard to rainfall variation.
4) Nest a regional climate model (RCM) within a limited subset of reanalysis or GCM output to provide insight into the benefits and shortcomings downscaling.
5) Develop plausible future climate scenarios for 2030-2050.

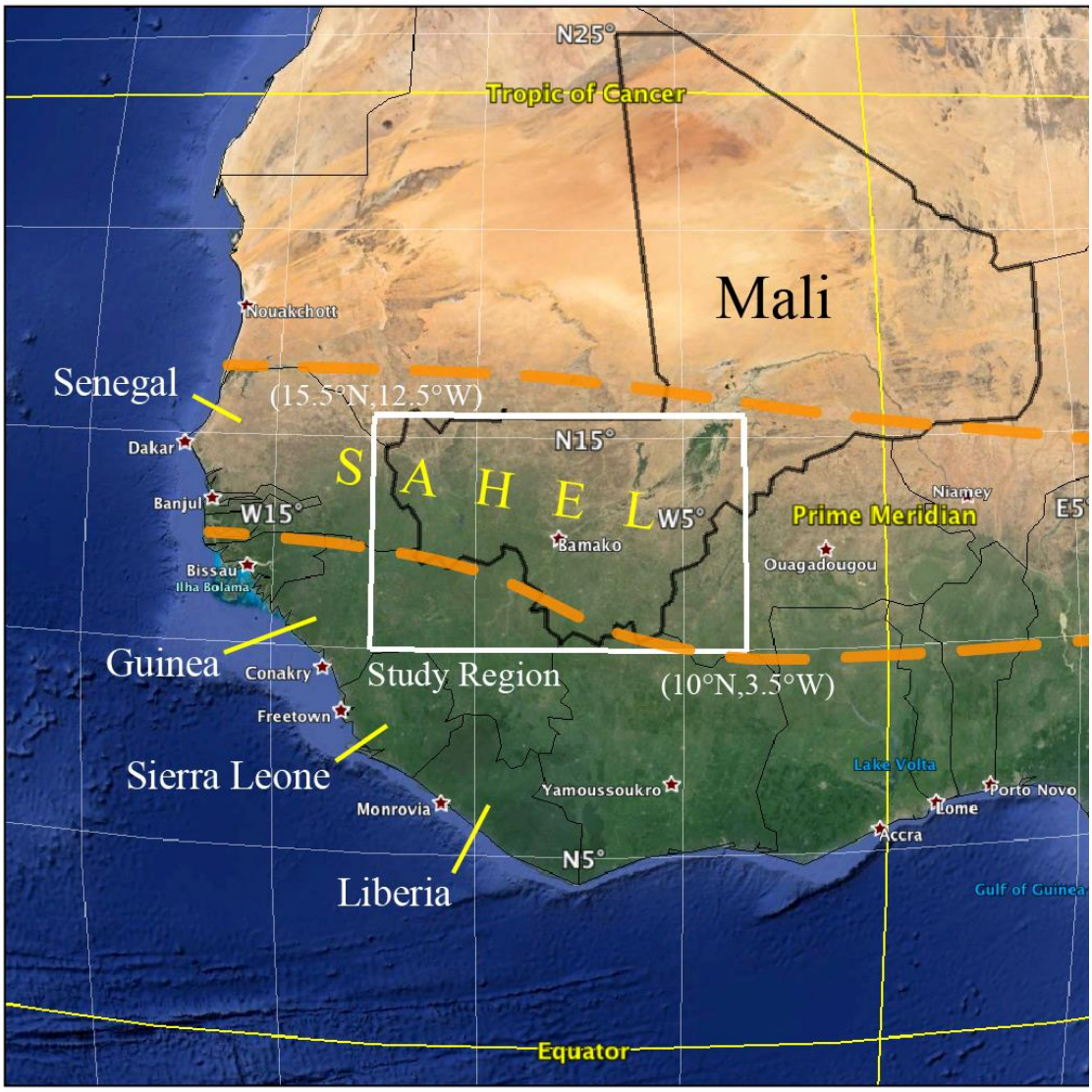

Figure 1. Location map depicting the study region (white box; 10°N -15.5°N, 3.5°W -12.5°W) centered on southwestern Mali in the West African Sahel (dashed orange lines). Basemap from Google Earth™.

Our findings are reported below in four sections covering historical climate trends (objectives 1 and 2), a synthesis of important climate teleconnections, future climate projections (objective 3), results and recommendations from a trial RCM downscale experiment (objective 4), and plausible future climate scenarios (objective 5). Particular attention is paid to the teleconnections section, where we elucidate how Mali's climate is impacted largely by North Atlantic SST variability through large-scale atmospheric circulation. These systems are in turn modified by radiative forcing from volcanic aerosols and human industrial emissions. Elsewhere we show that current GCMs are unable to validate against observations for the study region, thereby undermining the

fidelity of these models as predictive tools. Plausible future climate scenarios for Mali are therefore developed primarily on historical observations, teleconnections, and on a preliminary RCM downscale experiment.

Historical Trends from Gridded Observations and Reanalysis

Timeseries, Seasonal Cycle, and Spatial Context from Monthly Averages

In this section, we review the historical record of temperature and precipitation changes across a study domain spanning the monsoon-dominated, populous southern sector of Mali (Figure 1). This analysis uses two monthly gridded observational datasets, Global Precipitation Climatology Centre (GPCC) (Schneider et al., 2013) and the University of Delaware Air Temperature and Precipitation (UDATP) (Willmott and Matsuura, 2001). GPCC and UDATP are 0.25°x0.25° interpolations made from a global array of station data spanning the period 1901-2010. UDATP contains both precipitation and temperature estimates, whereas GPCC contains only precipitation. Here, we use temperature values from UDATP and precipitation values averaged from GPCC and UDATP.

Figure 2 shows annual temperature and precipitation anomalies for the southern Mali study region (i.e., Figure 1). From 1901 to 1970 temperature and precipitation exhibit low frequency variation (~ 20 year wavelength) without any distinct trend. The two variables are generally anti-correlated throughout the record period, such that cooler than normal temperature is associated with increased wetness, and warmer than normal temperature is associated with drought. This anti-correlation develops from thermal effects from cloud cover and strength of the monsoon (e.g., Martin and Thorncroft, 2014). The interval from the late 1960s to mid 1980s is marked by steep precipitation decline and temperature rise, constituting a significant drought. The prominent cool/wet (1950-1967) and warm/dry (1980-1997) intervals before and during the drought are highlighted in Figure 2 and referred to throughout this report. Partial rainfall recovery to values below the pre-1960s norm is found from the mid 1990s onward.

Figure 3 shows the temperature and precipitation annual cycles for the cool/wet and warm/dry intervals identified above. The difference in temperature between these periods is ~ 0.7 °C in April and May, and 0.5 °C in October. The occurrence of double thermal peaks in the annual cycle relates to lag response to tropical solar forcing, and to the onset of monsoon rain and cloud cover. The difference in August rainfall between the comparison periods is ~ 6.4 cm, or 22%.

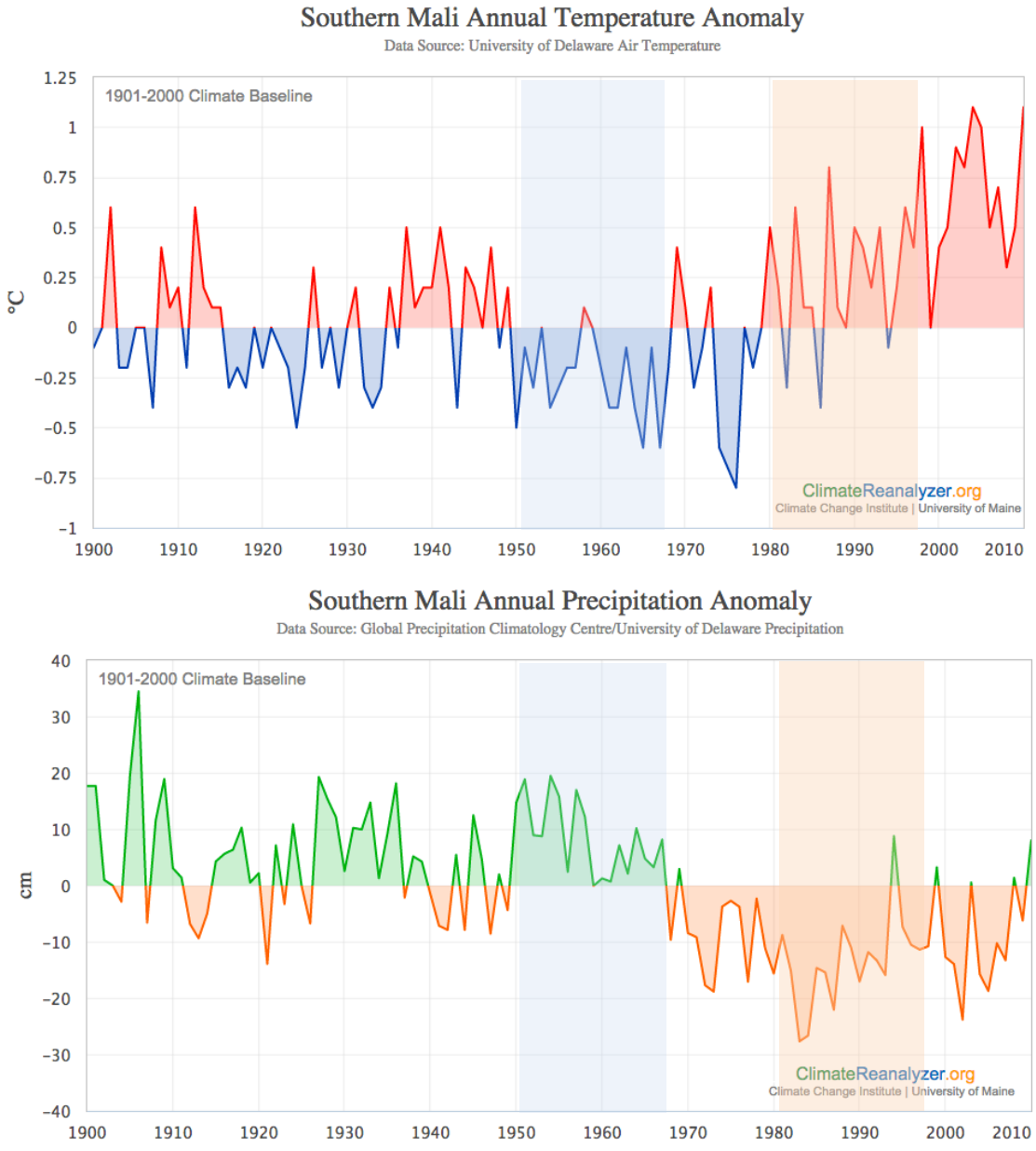

Figure 2. Annual mean temperature (top) and total precipitation (bottom) anomalies for Southern Mali for the years 1900-2010 from UDATP and GPCC gridded data. Blue and orange shading denote recent intervals of overall cool/wet (1950-1967) and warm/dry (1980-1997) conditions referred to throughout this report. Anomaly values based on 1901-2000 climatology. UDATP and GPCC data obtained from NOAA Earth System Research Laboratory (http://www.esrl.noaa.gov/psd/data/gridded/).

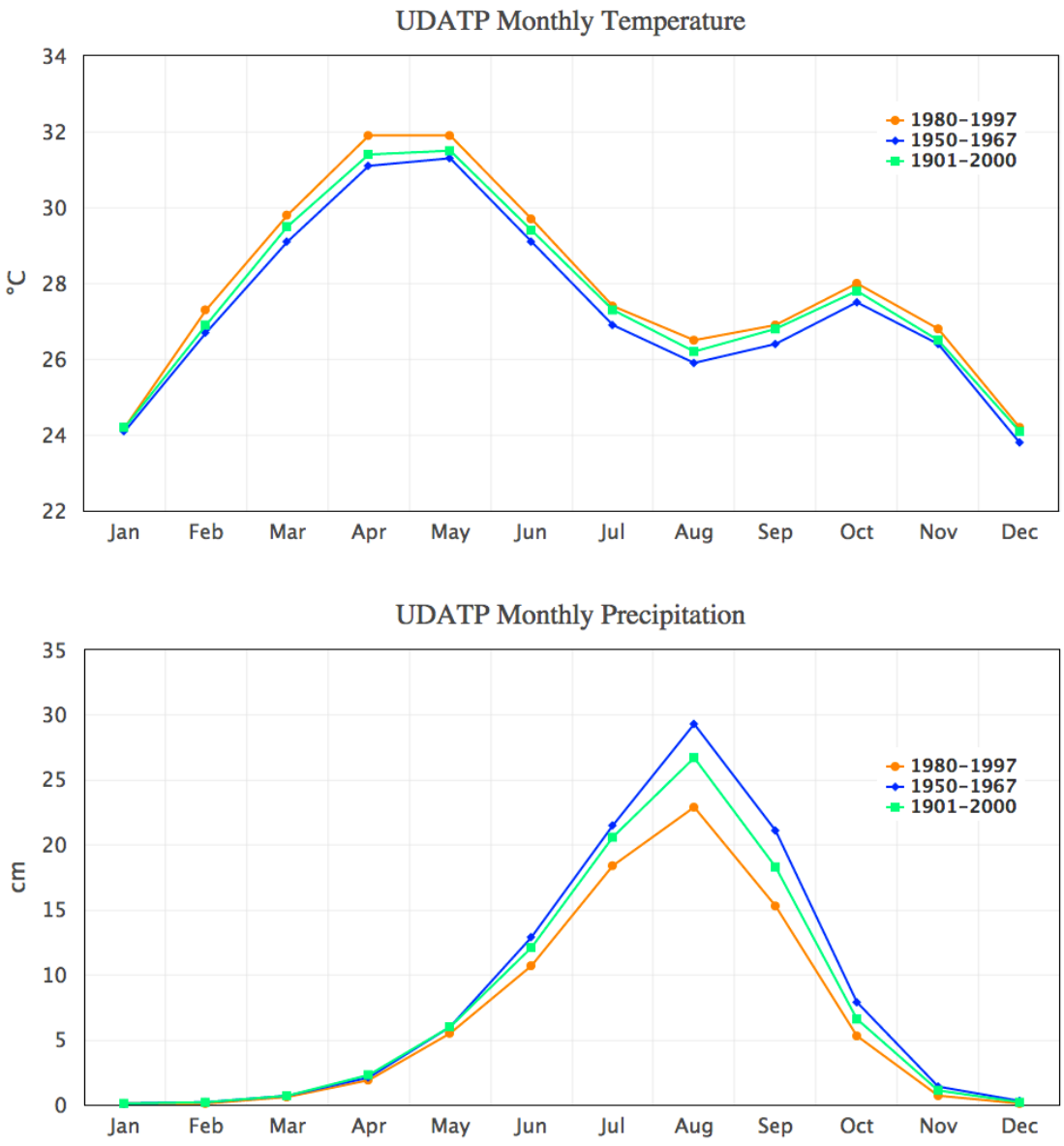

Figure 3. Annual cycles of mean temperature (top) and total precipitation (bottom) across Southern Mali for selected time periods from UDATP and GPCC gridded data.

Figures 4 and 5 show the spatial distributions of temperature and precipitation, and their respective anomalies. Of particular note is the plume of precipitation extending landward towards Mali from the southwestern coast between Senegal and Liberia. As noted earlier, this pattern emerges from the flow of onshore winds that develop with the arrival of the monsoon; a season of plentiful rainfall occurs when boundary conditions favor strong onshore circulation, whereas drought conditions prevail when this circulation is weak.

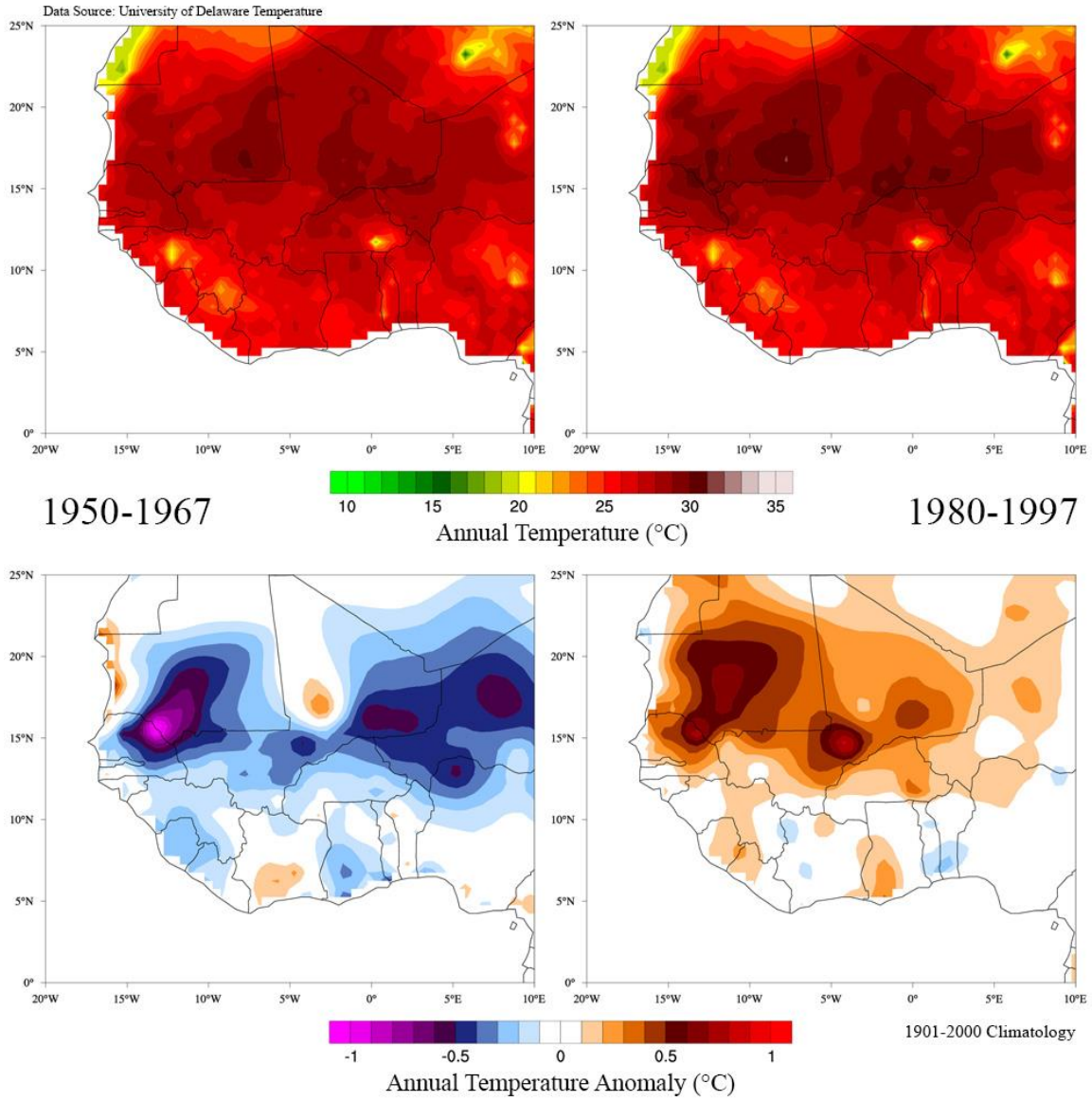

Figure 4. Mean annual temperature (top) and temperature anomaly maps (bottom) for 1950-1967 (cool/wet) and 1980-1997 (warm/dry) from UDATP gridded data. Anomaly values based on 1901-2000 climatology.

Frequency of Extreme Heat and Precipitation from Daily Reanalysis

In order to estimate changes in the frequency of heat and rainfall events over recent decades, we used daily maximum temperature and total precipitation output fields from the JMA 55-year Japanese Reanalysis model (JRA-55) (Ebita et al., 2011). JRA-55 is a state-of-the-art reanalysis with horizontal gridcell resolution of ~ 1°x1°. We chose JRA-55 for its relatively long timespan of 1958-present, which includes the latter part of Mali's mid-century wet climate. Other

comparable reanalysis models begin 1979. Reanalysis is used here because it provides an uninterrupted gridded measure of daily conditions across the study domain. To gauge the realism of JRA-55 across southern Mali, we compared monthly average temperature and precipitation output to the UDATP-GPCC gridded data used in the previous section. There is a strong correlation between reanalysis and observations for temperature (r=0.97), and moderate correlation for precipitation (r=0.49) (Figure 6).

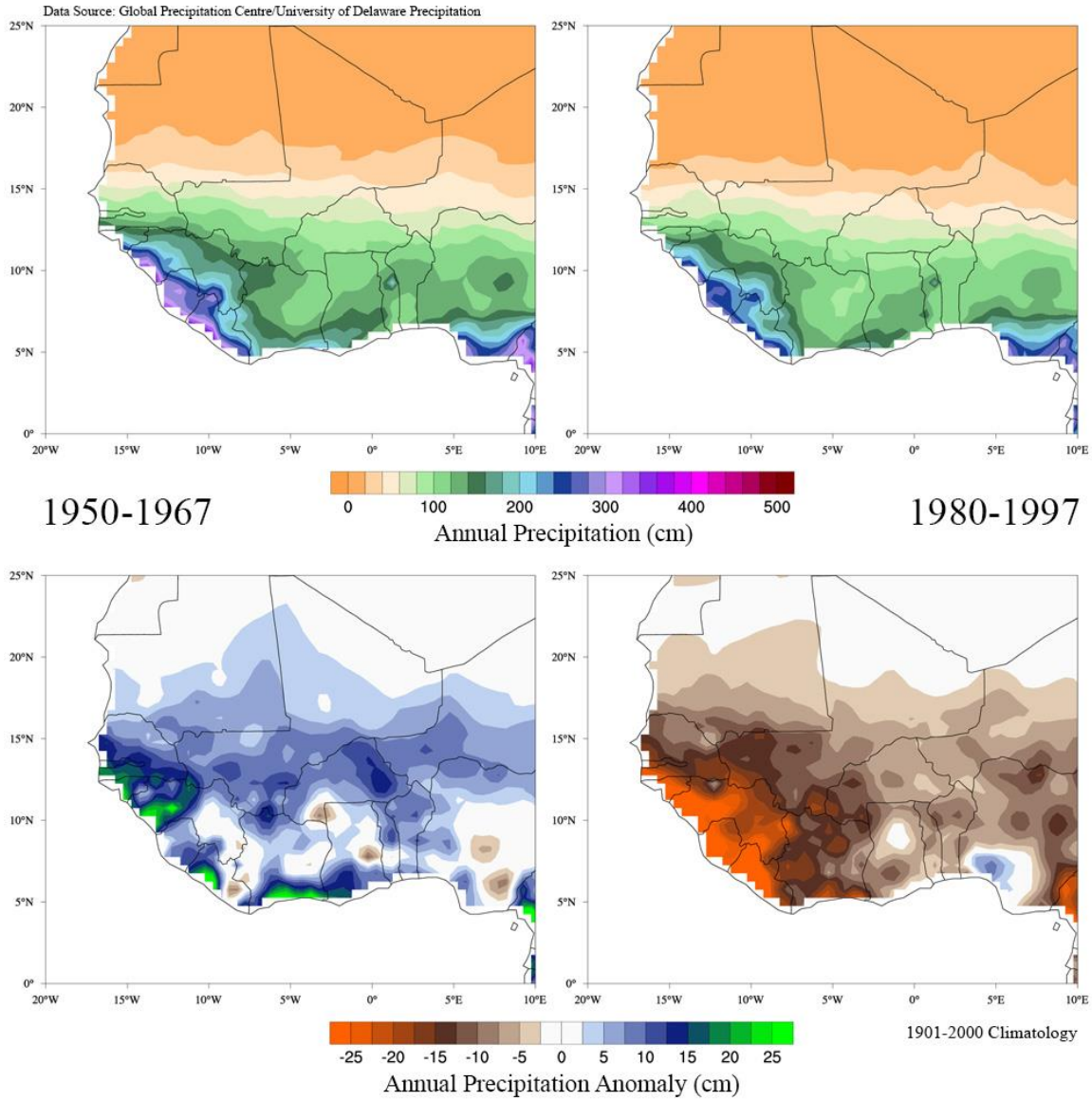

Figure 5. Total annual precipitation (top) and precipitation anomaly maps (bottom) for 1950-1967 (cool/wet) and 1980-1997 (warm/dry) from UDATP and GPCC gridded data. Anomaly values based on 1901-2000 climatology.

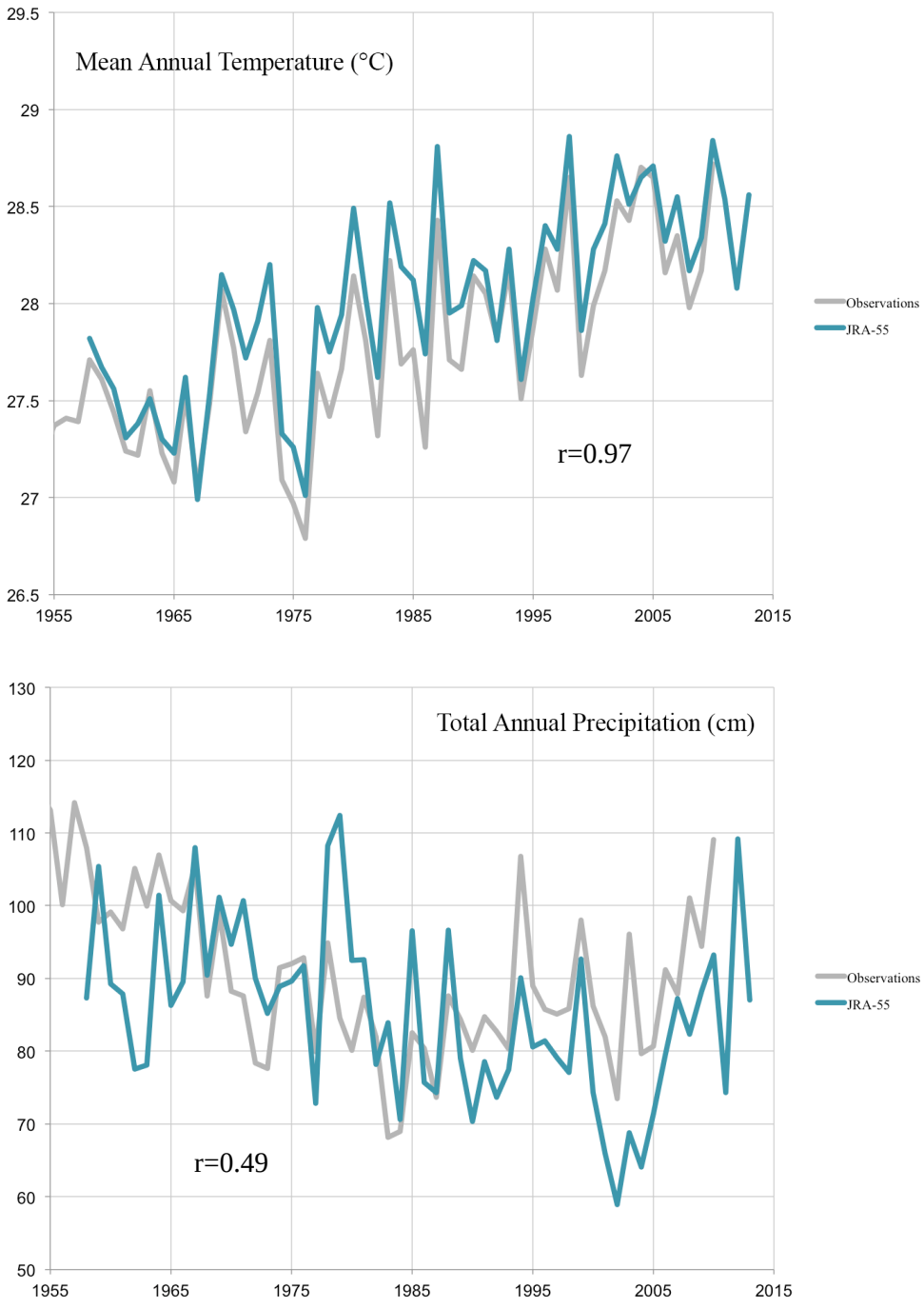

Figure 6. Timeseries comparison of JRA-55 reanalysis (gray line) and UDATP-GPCC gridded observations (blue-green line) for mean annual temperature (top) and total annual precipitation (bottom) averaged across Southern Mali.

Figure 7 shows heat and rainfall frequency charts. The results can be summarized as:

A) Number of days per year of prolonged heat, when the daily maximum temperature exceeds the 95th percentile of all values (38.5 °C, or ~101 °F). Since 1958, this metric has steadily increased on average from < 10 to ~ 30. The most extreme year of prolonged heat was 2010, when the 64 days met or exceeded the defined threshold.

B) Number of days per year of intense rainfall, when daily values are above the 95th percentile (79 mm). This metric shows a slight downward trend from 1958 to 1992, and an upward trend thereafter. Considerable interannual variability is found throughout. Since 2005, intense rainfall days have measured fewer (~ 10 days) than prior to about 1975 (~ 15 days).

C) Number of days per year of dryness, when daily precipitation is < 5 mm. This metric shows: ~ 195 annual incidences of dryness from ~ 1960 to 1975; a brief decline in dryness in the late 1970s; overall increase in dryness peaking in 2004 with ~ 250 incidences; and a marked decline in dryness (160 incidences in 2012) for the remainder of the record.

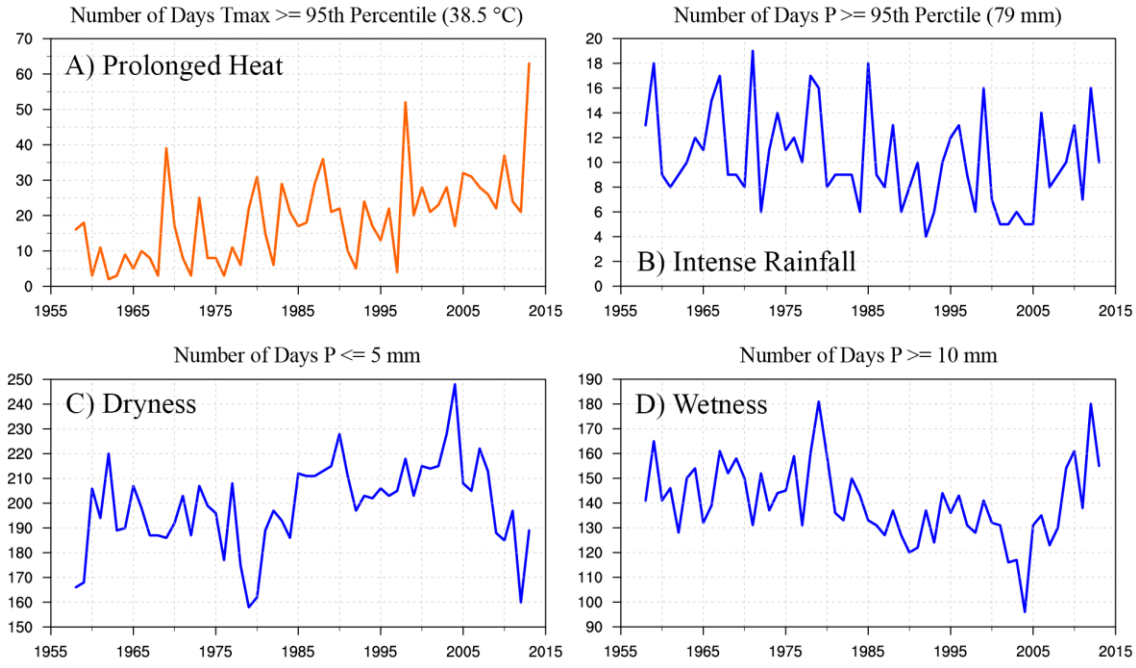

Figure 7. Metrics of heat and rainfall across Southern Mali derived from daily maximum temperature and total precipitation from JRA-55 reanalysis. Values are measured as the number of days per year beyond the specified threshold.

D) Number of days per year of wetness, when daily precipitation is >= 10 mm. The signal of this metric is an inversion of the dryness indicator in C. Perhaps most notable is the decline in this wetness metric between ~ 1980 and 2004, followed by a marked increase that peaks in 2012.

Teleconnections and Predictability of Mali's Climate

Mali's climate, and more broadly the WAM, is impacted on interannual timescales by several teleconnections, including the North Atlantic Oscillation (NAO) (Gaetani et al., 2011), El Niño–Southern Oscillation (ENSO) (Janicot et al., 2001), Atlantic Niño (Giannini et al., 2003), and conditions across the Mediterranean Sea (Rowell, 2003). Over longer timescales, the WAM is most strongly influenced by changes in SST (Lamb, 1978; Biasutti et al., 2009). Mohino et al. (2010) show from a suite of GCM experiments with prescribed SSTs that the Atlantic Multidecadal Oscillation (AMO), Inter-decadal Pacific Oscillation (IPO), and anthropogenic warming of tropical oceans together describe most of the historically observed low-frequency variation in Sahelian rainfall. The authors further ascribe 50% of the SST-driven drought between ~ 1965 and 1985 to onset of the cool phase of the AMO, and link the subsequent partial rainfall recovery across the region to re-emergence of the AMO warm phase and increased anthropogenic warming. Other workers have also linked the observed limited rainfall recovery to human causes (e.g., Zeng, 2003; Gioninni et al., 2008; Rodriguez-Fonseca et al., 2011).

The noted importance of the AMO in modulating Mali's climate warrants further discussion of the phenomenon. The AMO is the dominant mode of SST variability in the North Atlantic, typically represented in time as the de-trended signal of average temperature from 0°N to 70°N (Enfield et al., 2001) (Figure 8). Cool and warm intervals of the AMO span ~ 30 years and are associated with changes in sea-level pressure and large-scale atmospheric circulation (Grossman and Klotzbach, 2009). The precise dynamical origin of the AMO is not yet known. Possible mechanisms include internal ocean variability, either natural (Knight et al., 2005; Jungclaus et al., 2005) or modified by anthropogenic forcing (Mann et al., 2015), and coupled ocean-atmosphere response to external forcing from solar variability and volcanic and anthropogenic aerosol emissions (Booth et al., 2012; Knudsen et al., 2014).

Rainfall across the western Sahel is coupled to the AMO through large-scale atmospheric circulation. Figure 9 shows maps of wind, pressure, and SST across the North Atlantic for Mali's cool/wet (1950-1967) and warm/dry (1980-1997) intervals identified previously in Figure 2.

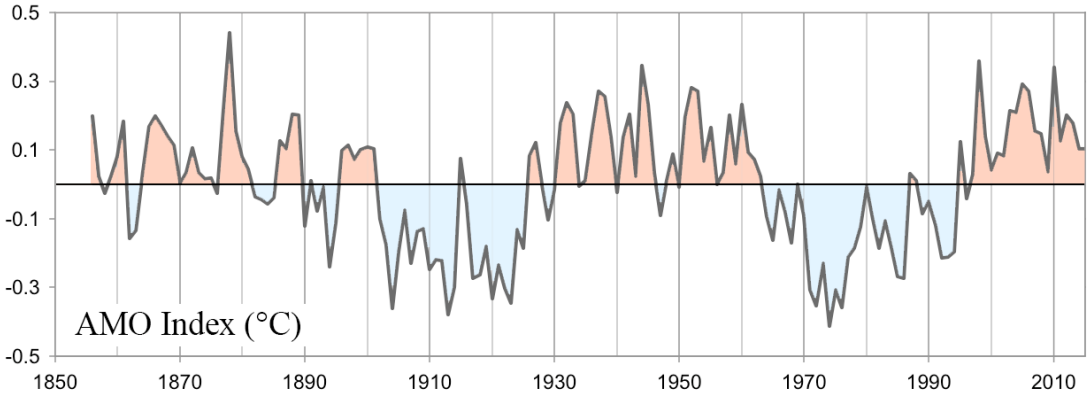

Figure 8. The Atlantic Multidecadal Index (AMO) with warm and cool intervals shaded red and blue, respectively. Data from NOAA Earth System Research Laboratory (http://www.esrl.noaa.gov/psd/data/timeseries/AMO/).

These intervals overlap AMO-warm and AMO-cool, respectively. The mean atmospheric pattern coincident with AMO-warm is that of relatively weak wind and shallow pressure gradient between the Azores High and Icelandic Low. Conversely, AMO-cool is coincident with relatively strong wind and steep poleward pressure gradient. These opposing circulation regimes define respective modes of the atmospheric NAO. A key distinction between these two conditions is either strong or weak development of the Sahara Low, a pressure center coupled to onshore circulation, the WAM, and to the latitudinal position of the ITCZ (Figure 10). Thus, rainfall is abundant across southern Mali when North Atlantic SSTs are warm and large-scale atmospheric circulation is weak, whereas drought occurs when SSTs are cool and circulation is strong.

What drives the AMO?

Mali's future climate will depend in large part on the evolution of the AMO, and its impact on strength of the Sahara Low and position of the ITCZ. The dominant scientific paradigm holds that the AMO is coupled dynamically to Atlantic Meridional Overturning Circulation (AMOC) (e.g., Knight et al., 2005; Jungclaus et al., 2005). AMOC consists of the northward flow of warm, salty surface waters into the high latitudes of the North Atlantic via the Gulf Stream and North Atlantic Current, and the southward return flow of cold water at depth (Rahmstorf, 2002). It is widely thought that AMOC can slow, or cease altogether, when major plumes of freshwater enter

the vicinity of southern Greenland, where changes in buoyancy impede downwelling and the production of North Atlantic Deep Water. This process is commonly implicated in abrupt climate cooling episodes registered during glacial times (Clark et al., 2001). Arctic warming and

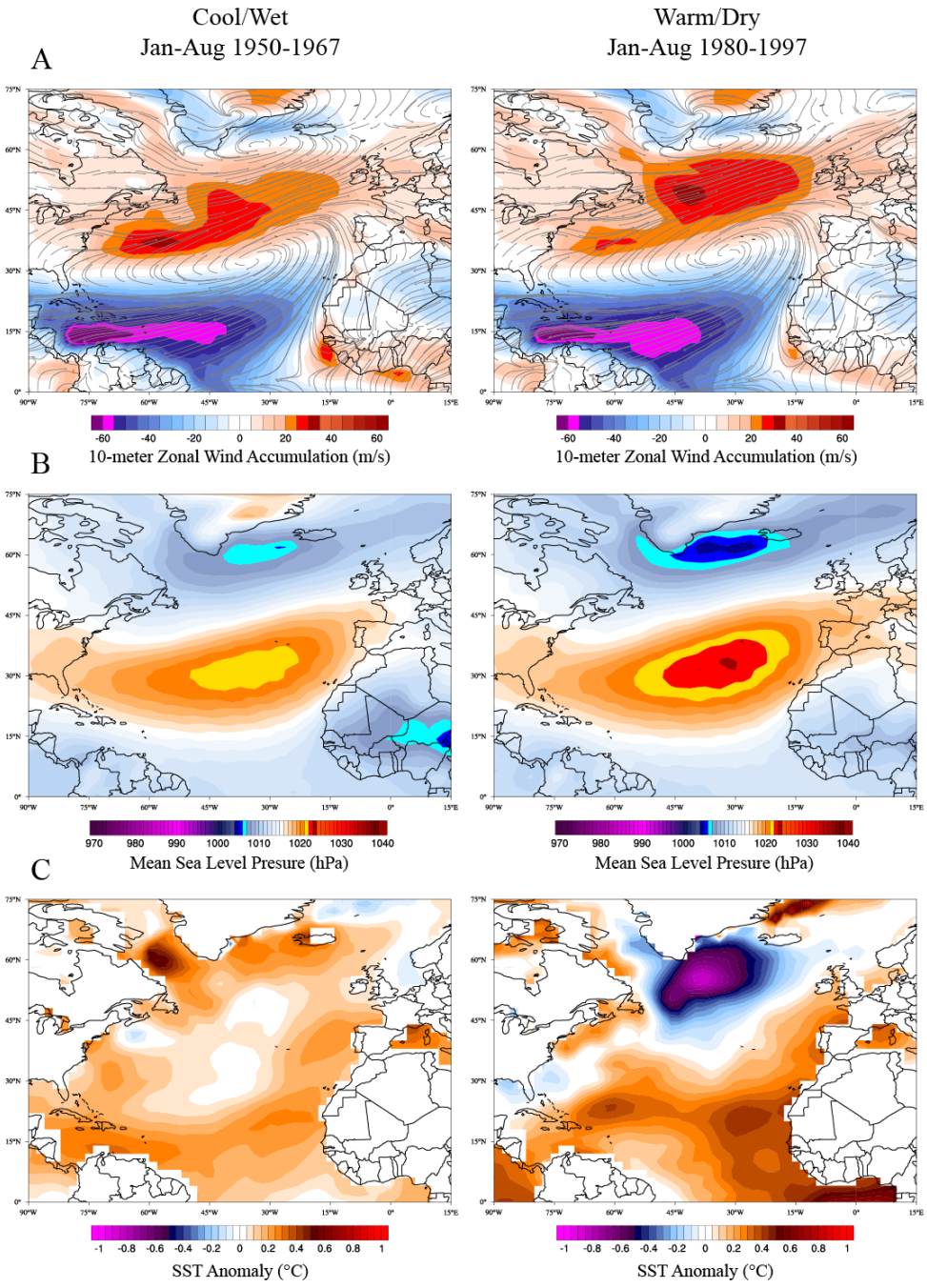

Figure 9. North Atlantic region comparison of January-August A) accumulated 10-meter zonal (west-east) wind with wind speed vector overlay, B) mean sea level pressure, and C) SST anomaly (1901-1980 climatology) for the Mali cool/wet and warm/dry periods identified in the text. Atmospheric fields in A and B are from NCEP/NCAR Reanalysis (Kalnay et al., 1996), and the SST fields in B are from NOAA ERSST version 3b. Output files obtained from NOAA Earth System Research Laboratory (http://www.esrl.noaa.gov/psd/data/gridded/) and maps generated using UM-CCI Climate Reanalyzer (http://cci-reanalyzer.org).

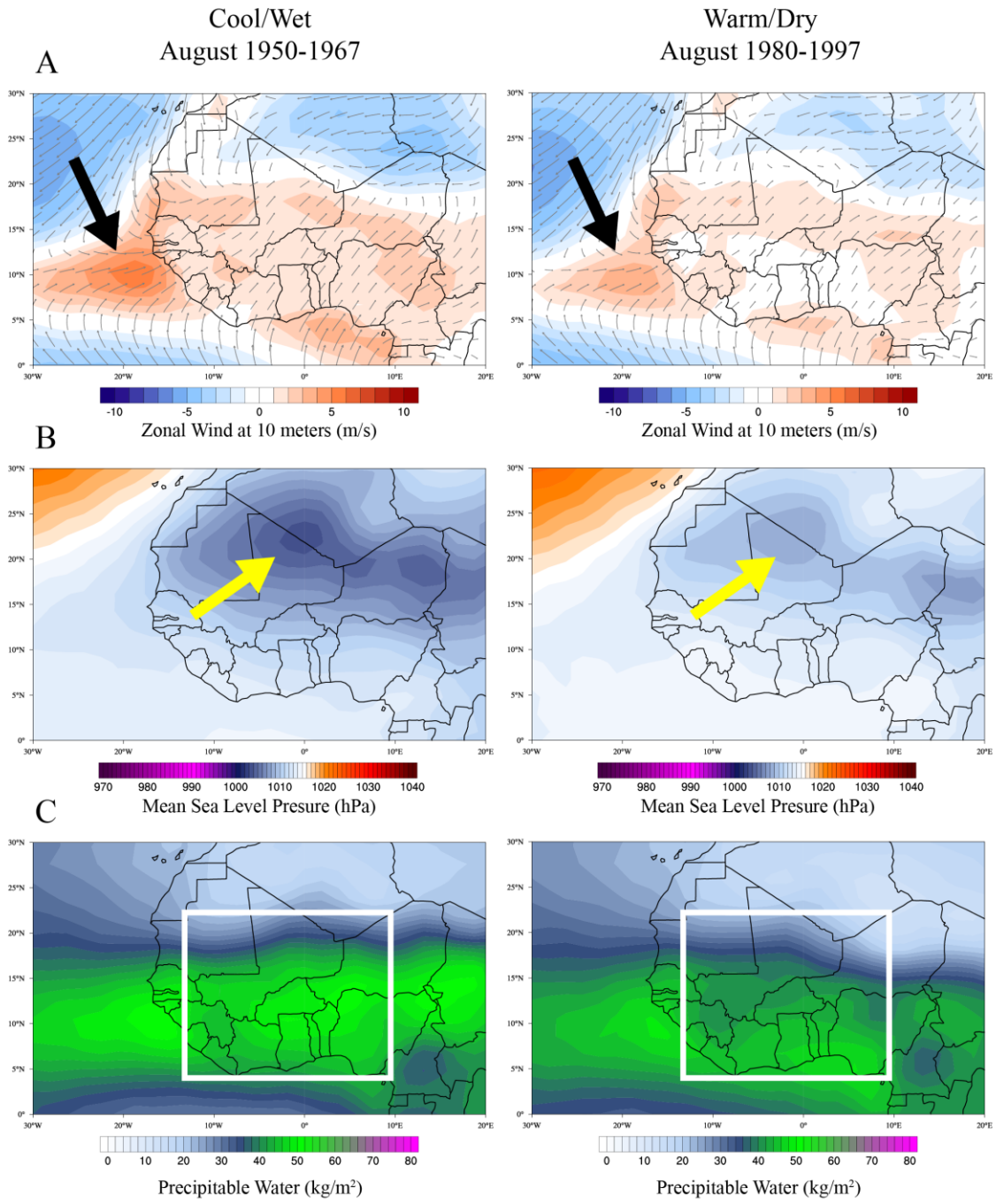

Figure 10. Comparison of A) zonal wind, B) mean sea-level pressure, and C) precipitable water for West Africa from NCEP/NCAR Reanalysis. The left column shows cool/wet (1950-1967) conditions across the Western Sahel, warm/dry (1980-1997). Arrows in A and B highlight important circulation features that are different in the two climate regimes, including the Sahara Low in the pressure field. The white box in C is for emphasis on the region that sees greatest moisture surplus or deficit. Maps generated using UM-CCI Climate Reanalyzer (http://cci-reanalyzer.org).

subsequent meltwater production is likewise suggested to pose uncertainty for projections of future climate (Rahmstorf et al., 2015). An alternative viewpoint postulates that AMOC is driven more fundamentally from atmospheric wind-stress, and that buoyancy forcing is secondary or insignificant (Wunsch, 2005; Clement et al., 2015).

We favor atmospheric forcing mechanisms for the AMO and AMOC. Perhaps the most compelling evidence to this end is the decisive overlap between cool intervals in the North Atlantic and episodes of high volcanic activity as identified from aerosol optical depth in the atmosphere (Figure 11). Previous authors have noticed this relationship as well, and have suggested that the oceanic system responds to changes in atmospheric circulation manifested through the NAO (Shindell et al., 2004; Knudsen et al., 2014). Indeed, observations show that the Northern Hemisphere atmospheric response to a major volcanic eruption resembles NAO-negative (strong winds, steep poleward pressure gradient) (Driscoll et al., 2012). This behavior is consistent with NAO-positive type circulation that we find coincident with the cool phase of the AMO, a weakened Sahara Low, and warm/dry conditions across southern Mali (i.e., Figures 9 and 10).

A wind-stress AMOC linkage is shown in Figure 12. Here, it is evident that SST in the subpolar North Atlantic (50°N-60°N, 55°W-10°W) co-varies with the speed of overlying winds and the pressure difference between Azores and Iceland (Figure 12a-c). That SST anomalies in this region respond to wind forcing can be inferred from the steep signal adjustment mid-1990s, wherein wind and pressure appear to lead temperature by one year. Further large-scale teleconnection is evident from the close correspondence between subpolar SST, wind speed, and precipitation across Mali (Figure 12d), where westerly wind speed increases as SST and Sahelian rainfall decline. Mid-century Sahelian drought and subsequent partial rainfall recovery is also well represented by changes in mean jetstream winds averaged across the Northern Hemisphere from 30°N-60°N (Figure 12e).

In all, atmospheric circulation, and the westerlies in particular, play a fundamental role in North Atlantic SST variability, latitudinal position of the ITCZ, and strength of the Sahara Low and WAM. The predictability of Mali's future rainfall will therefore depend strongly on our understanding of the processes governing wind and pressure patterns across the North Atlantic and other world ocean basins. Anthropogenic warming of tropical SSTs is one mechanism for increasing the poleward gradient and strengthening winds (e.g., this could underpin the

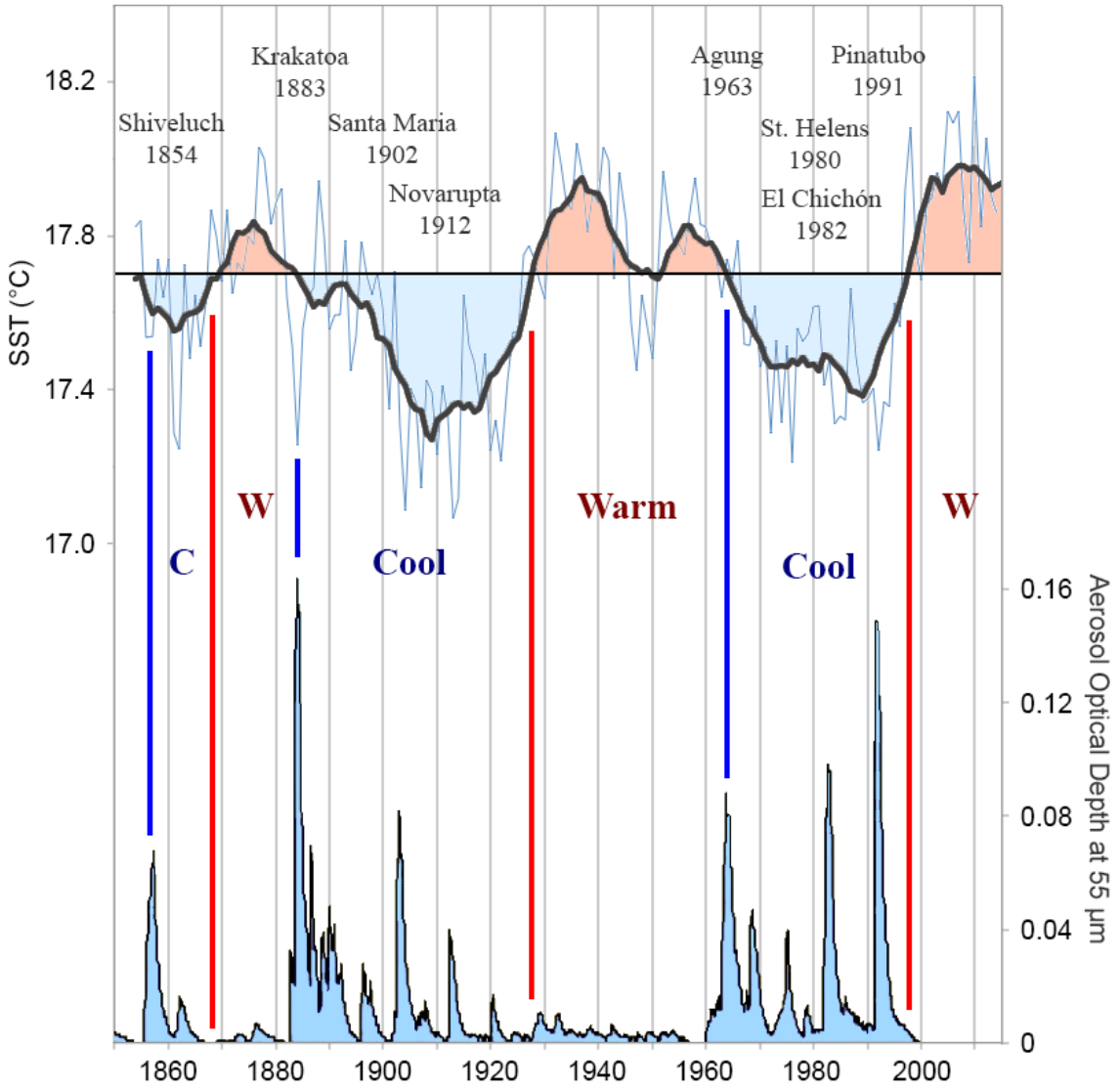

Figure 11. Comparison of the AMO index to aerosol optical depth. Major volcanic eruptions corresponding to aerosol spikes are labeled. Aerosol optical depth data from NASA GISS (http://data.giss.nasa.gov/modelforce/strataer/).

hemispheric wind signal in Figure 12e). A second mechanism is stratospheric ozone depletion, a human-caused phenomenon known to have caused speedup and poleward migration of the Southern Hemisphere westerlies around Antarctica over the past 30 years (Perlwitz et al., 2008; Polvani et al., 2011; Lee and Feldstein, 2013). The impact of stratospheric ozone depletion on Northern Hemisphere circulation is less understood, mainly because of smaller ozone losses over the Arctic compared to Antarctic, and from greater meteorological variability in response to land-sea contrasts. We nevertheless speculate that the northern westerlies may have strengthened and

shifted poleward in response to ozone changes (i.e., Hartmann et al., 2000), in part explaining the timeseries trends shown in Figure 12. A third mechanism for changing large-scale wind and pressure patterns is Arctic sea-ice decline, which has accelerated since ca. 2000 coupled to a slowdown of the westerlies (Francis and Vavrus, 2015).

Future Climate Projections

Future climate projections computed by GCMs as part of the CMIP5 program are widely used for climate adaptation and planning. These models are sophisticated numerical frameworks that provide useful insight into how the global climate system may evolve in response to changing boundary conditions affected by humans. Figure 13 shows projected changes in the annual cycle for temperature and precipitation across Southern Mali. Here, we used ensemble-average output from the NCAR CCSM4, a leading model in CMIP5, for the periods 1901-2000 (century-long climatology), 1950-1967 (cool/wet in observations), 1980-1997 (warm/dry in observations), and 2050-2067. Historical solutions include estimated radiative forcing from volcanic eruptions, solar variability, and anthropogenic aerosol and greenhouse-gas emissions. The future projection is from the Representative Concentration Pathway (RCP) 8.5 experiment, which can be understood as the highest greenhouse-gas emissions scenario. Taken at face value, this case projects about 2 °C warming and negligible change in total annual precipitation between the recent climate of 1980-1997 and ca. 2050. Temperature change is distributed homogenously across the year, while peak precipitation shifts from August to September.

Comparison of GCMs to Observations

The fidelity of future projections can be gauged by the ability of a GCM to reproduce observed historical climate. In this vein, we note that annual cycles in CCSM4 depart from observations in significant ways (Figure 13). First, CCSM4 temperature has a cold bias of ~ 2 °C from January to May spanning the first thermal peak of the year. Second, precipitation is anomalously high from March to May, and anomalously low from June to August, which in all produces an asymmetrical annual rainfall signal. Observations show rainfall peaking in August with a symmetrical buildup and decline. Peak rainfall in CCSM4 is ~ 25% lower than in observations.

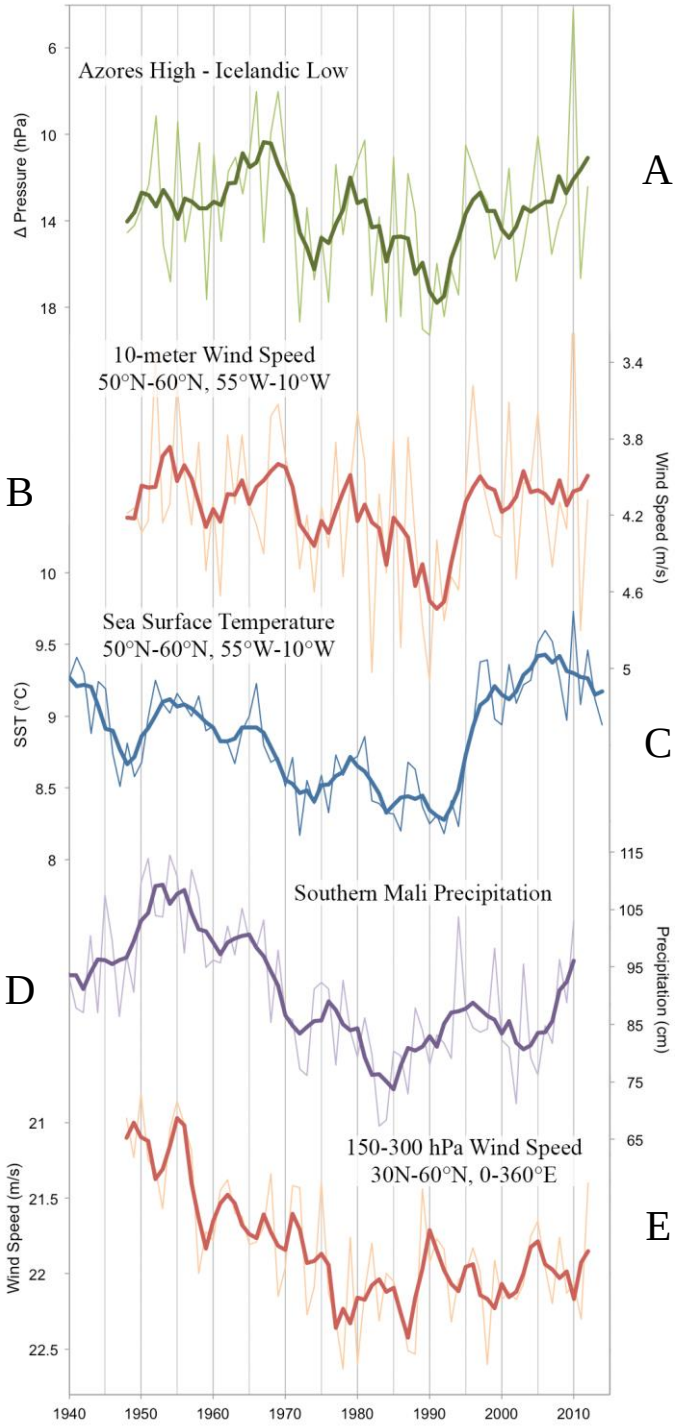

Figure 12. Annual timeseries stack for A) difference in pressure between Azores and Iceland, B) average wind speed at 10 meters above the surface for an area south of Greenland, C) SSTs across the same area in B, D) precipitation across Southern Mali, E) average wind speed over the Northern Hemisphere middle latitudes from 30-60°N. A, B, and E from NCEP/NCAR Reanalysis; C from NOAA ERSST; D from UDATP/GPCC.

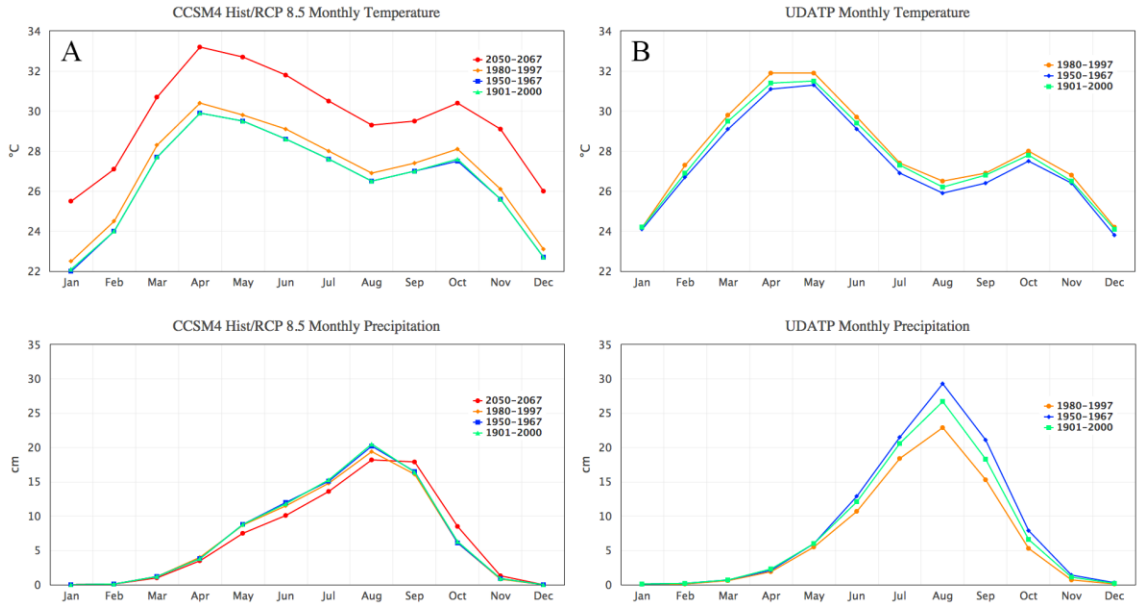

Figure 13. Annual cycles of mean temperature (top) and total precipitation (bottom) across Southern Mali for selected time periods for A) CCSM4 Historical and RCP 8.5 simulations and B) UDATP observations. CCSM4 output obtained from Earth System Grid (https://www.earthsystemgrid.org) and UM-CCI Climate Reanalyzer (cci-reanalyzer.org).

Further disagreement with observations is found from both CCSM4 and the multi-model CMIP5 temperature and precipitation annual timeseries (Figure 14). Here, in addition to cold bias and precipitation deficit, the GCM signals lack distinct multi-decade variability. Signal mismatch is emphasized in Figure 15 for a single ensemble member of CCSM4, where the GCM shows upward-trending temperature and flat-lined precipitation throughout the 20th century, whereas observations show low-frequency changes in both metrics with no apparent upward (temperature) or downward (precipitation) trends until after ~ 1970.

Finally, we determine that large-scale atmospheric circulation is considerably stronger in the GCM than in reanalysis (Figure 16). An unrealistically steep pressure gradient and strong winds across the North Atlantic may account for a weak simulated monsoon. Other authors have noted a lack of GCM realism in simulating the WAM (Rodriguez-Fonseca et al., 2011). On the contrary, Giannini et al. (2008) show that observed Sahelian rainfall anomalies can be simulated in a GCM, but only with prescribed SSTs, and not with SSTs from a dynamically-coupled ocean model. Coupled ocean-atmosphere GCMs also fail to reproduce observed NAO response to volcanic forcing and multi-decade variability (Driscoll et al., 2012). This suggests to us that coupled ocean models within CMIP5 may be important sources of error. Thus, projected changes

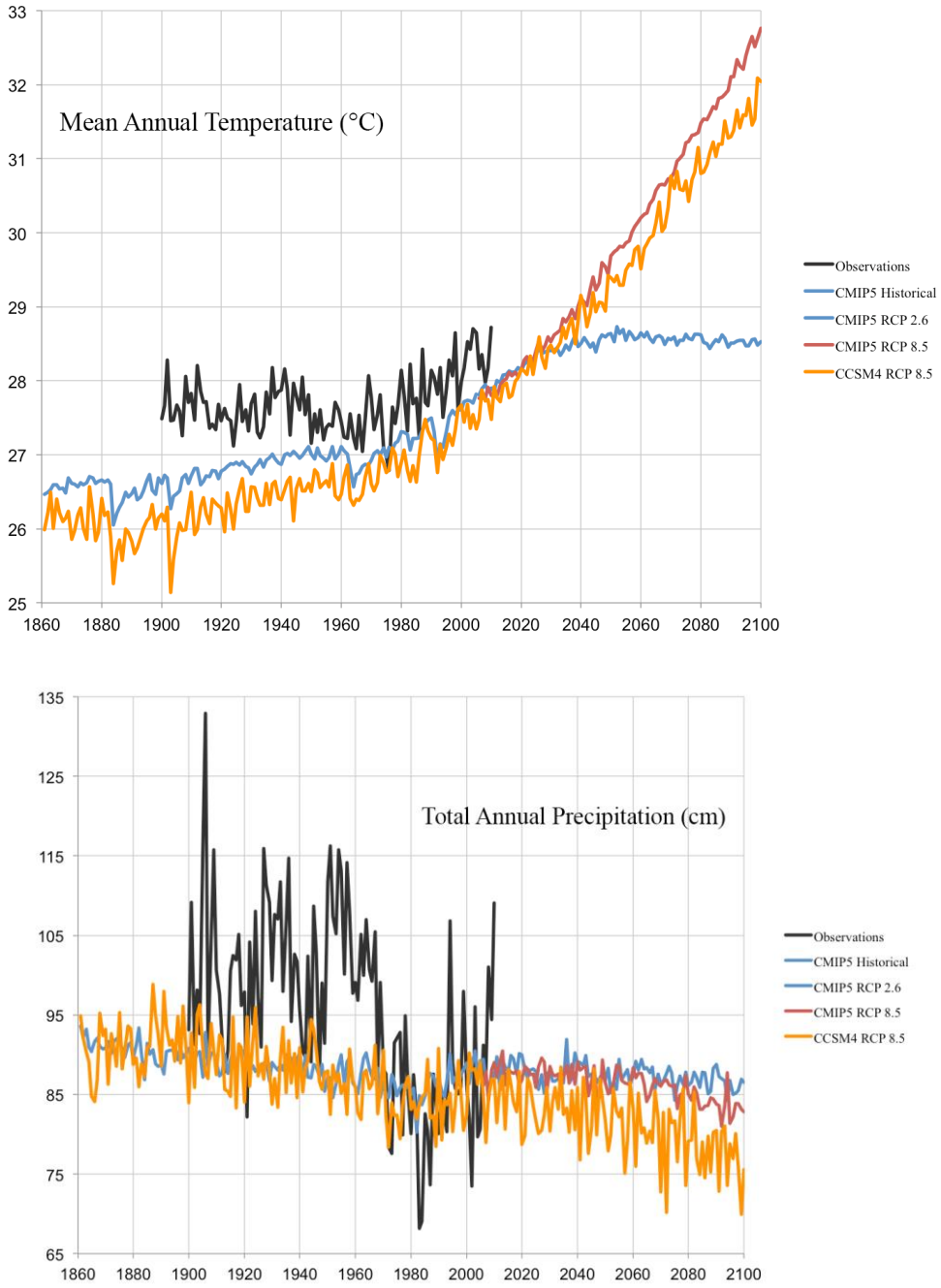

Figure 14. Comparison of mean annual temperature (top) and total annual precipitation (bottom) for UDATP-GPCC gridded observations (black), CMIP5 historical multi-model ensemble average (blue; 1861-2005), CMIP5 RCP 2.6 multi-model ensemble average (blue; 2006-2100), CMIP5 RCP 8.5 multi-model ensemble average (red; 2006-2100), and CCSM4 RCP 8.5 single-model ensemble average for Southern Mali. CCSM4 output obtained from Earth System Grid (https://www.earthsystemgrid.org) and UM-CCI Climate Reanalyzer (cci-reanalyzer.org). CMIP5 output obtained from KNMI Climate Explorer (http://climexp.knmi.nl).

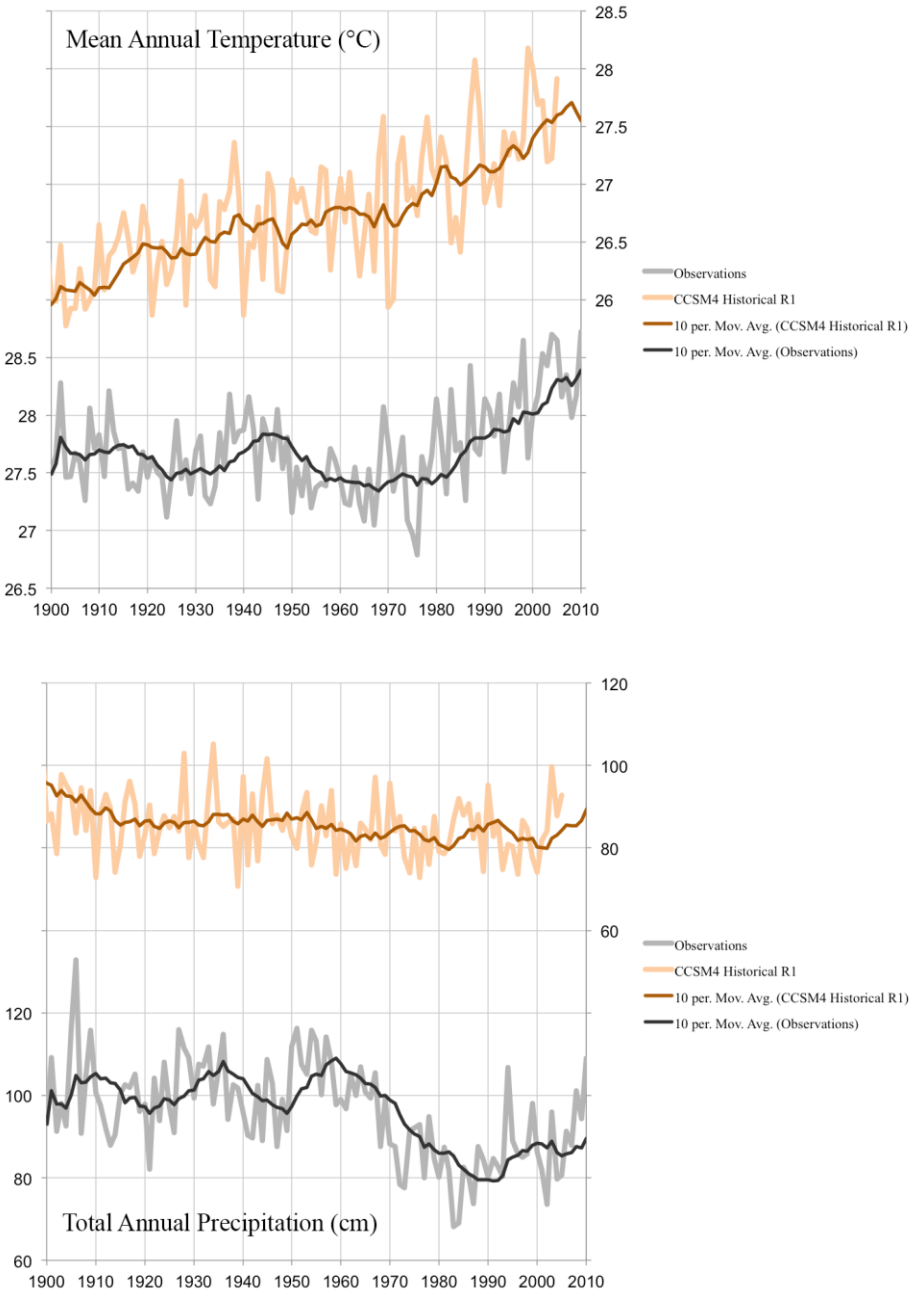

Figure 15. Comparison of mean annual temperature (top) and total annual precipitation (bottom) for UDATP-GPCC gridded observations (black) and the first ensemble member of the CCSM4/CMIP5 historical run for Southern Mali. CMIP5 output obtained from KNMI Climate Explorer (http://climexp.knmi.nl).

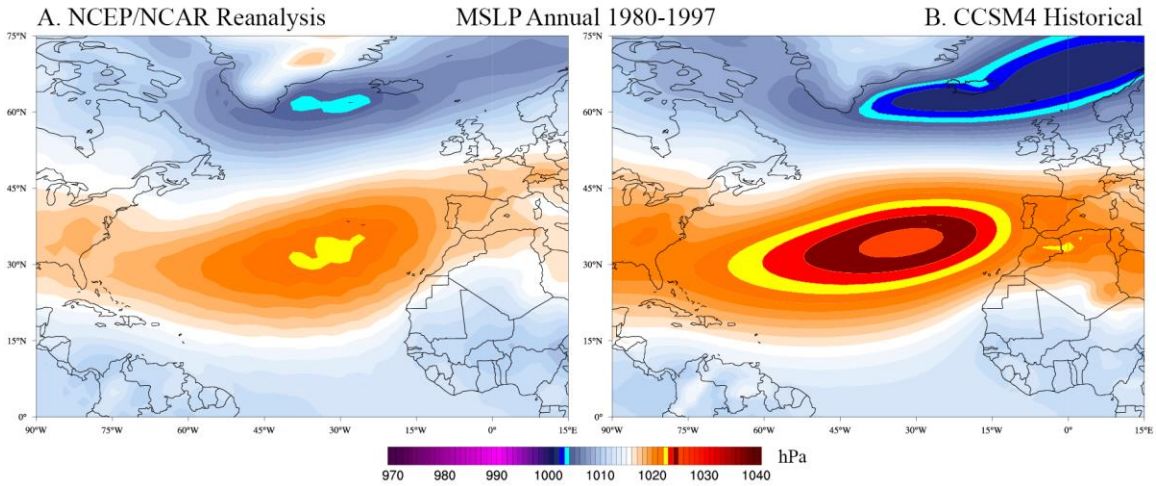

Figure 16. Comparison of annual mean sea-level pressure across the North Atlantic basin calculated in A) NCEP/NCAR Reanalysis and B) CCSM4 Historical for the period 1980-1997. Maps generated using UM-CCI Climate Reanalyzer (http://cci-reanalyzer.org).

to temperature and rainfall across Southern Mali may have ambiguous meaning in the current generation of CMIP5 models.

Regional Downscale Model Trial

We conducted an exploratory experiment using a Regional Climate Model (RCM) to provide insight into the benefits and shortcomings of downscaling. "Downscaling" refers to the process of nesting a regional climate model (5-25 km horizontal grid resolution) into reanalysis or a GCM (50-250 km) to produce a dynamical solution with regional-to-local scale information. RCMs afford greater skill than coarse models in representing a variety of meteorological processes, including resolution-limited processes such as orographic and convective precipitation. RCMs are most widely used to improve short-term weather forecasts, but have also been used in recent years in analyses of GCM-projected climate (Liang et al., 2008).

In this exercise we downscaled a subset of ERA-Interim (ERAI) reanalysis in a 30/10 km domain nest (Figure 17) centered on Mali using version 3.5.1 of the Weather Research and Forecasting (WRF) model (Skamarock et al., 2008). Reanalysis was chosen for lateral boundary forcing in order for the downscale result to be compared directly against observations. The simulation was run from May 1st to October 31st for 1994, as an example of a strong monsoon year. The

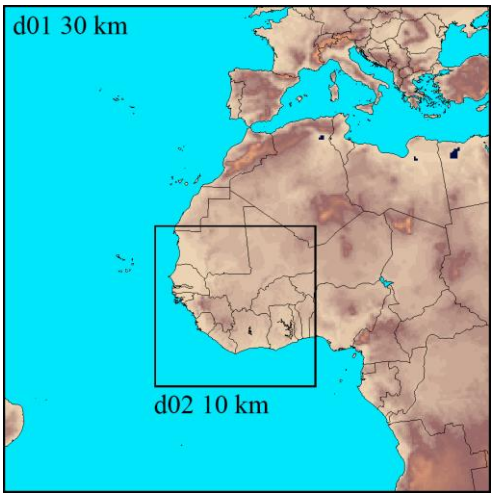

Figure 17. WRF domains used in downscale exercise.

relatively coarse outer domain was a necessary intermediate step in translating heat and moisture fluxes from ~ 80 km reanalysis down to 10 km. The latter domain is sufficient resolution for explicit convective precipitation, which is important for monsoon simulations (Garcia-Carreras et al., 2015). See Table 1 for chosen model physics options.

Figure 18 shows downscale results compared against ERAI and observations for daily maximum temperature and accumulated precipitation over Sikasso, Mali (11.3°N, 5.6°W). It is evident that reanalysis temperature (Figure 18A) is consistently cooler than observations by ~ 2 °C, while exhibiting overall pattern match and the highest correlation to observations, r=0.91. Both downscale simulations improve temperature agreement with observations from mid June thru September; however, significant warm biases are found for May thru early June (2-4 °C) and again in October (1-2 °C). Correlation to observations is only moderate for the downscale simulations, where r=0.68 for the 30 km outer domain and r=0.65 for the 10 km nest. The reanalysis accumulated precipitation similarly best approximates observations (Figure 18B; see also Figure 19 for spatial comparisons). It is surprising that the convection-permitting 10 km downscale nest has the poorest fit, with total accumulated precipitation ~ 30% greater than observations. These results suggest the need for detailed sensitivity testing in order to determine precisely what physics options are necessary for optimum performance of WRF over West Africa.

Considerations and Recommendations

GCM downscaling is widely sought after for studies of future climate impacts that require local-scale information (e.g., surface and meteorological fields for agricultural crop models). However, there are important factors to consider before investing resources in such an undertaking. First, RCMs require sensitivity testing and tuning in order to attain optimum realism for a given region. This validation must be done against observations in order to identify and reduce biases in important metrics such as temperature and precipitation. Second, downscale models are limited

by the robustness of lateral and lower boundary forcing from the coarse input models. Thus, experiments should use a GCM that closely reproduces historical climatology for the study region. Without historical validation there is not a means to ascribe fidelity to future projections.

In the case of Southern Mali, we find that the CMIP5 multi-model ensemble average and CCSM4, a leading model within CMIP5, fail to reproduce key aspects of observed historical temperature and precipitation variability across Southern Mali. We furthermore find that large-scale circulation across the North Atlantic is anomalously strong in CCSM4 compared to reanalysis. Given a key finding in the teleconnections section – namely, that strength of the West African Monsoon carries a strong dependency on large-scale circulation – we are hesitant to downscale a GCM that does not adequately reproduce crucial boundary conditions. Any result from such an experiment, whether projecting drought frequency or storm intensity, would have ambiguous meaning.

In considering the above points, we recommend the following experiment templates that could provide useful inputs for agricultural crop modeling, and further insight into Mali's future climate:

- Downscale reanalysis for years of extreme warmth/dryness (2004) and extreme warmth/wetness (2010). These cases can be used to represent plausible scenarios of future average conditions.

- For the cases above, change SST (e.g., warm the surface waters within the simulation domain by +0.5 or +1.0 °C) in a series of sensitivity tests to evaluate the impact on monsoon development.

- Initiate a program of weekly or monthly high-resolution downscaling of 2-5 month climate outlook models (e.g., the NOAA/NCAR Climate Forecast System [CFS] Model). This could provide useful information for agriculture stakeholders weeks or months in advance of the monsoon.

- Undertake a rigorous examination of all available GCMs within CMIP5 to determine which model presents the most realism for pressure and wind across the North Atlantic basin, and for reproduction of the observed annual cycle across Mali. A validated model could then be downscaled with some confidence.

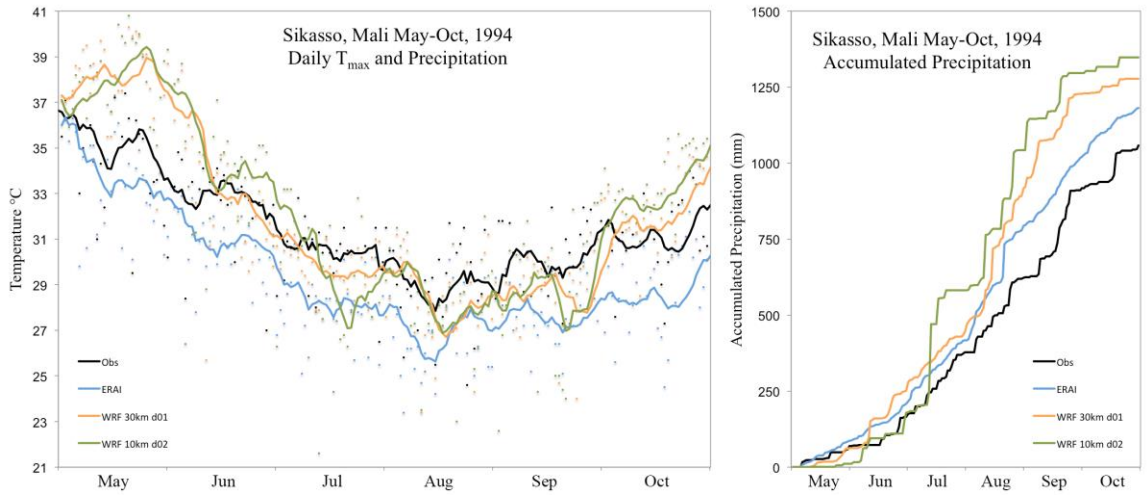

Figure 18. Observations (black), ERA-Interm reanalysis (blue) and timeseries results from WRF downscale simulations (30 km, orange; 10 km, green) for daily maximum temperature (left) and accumulated precipitation (right) for Sikasso, Mali (11.3°N, 5.6°W), May 1st to October 31st, 1994. Bold lines in left panel indicate 10-day running mean for temperature.

Conclusions and Plausible Future Climate Scenarios

We examined historical data, reanalysis, general circulation models, and a regional climate model in order to provide insights into Mali's historical and projected climate variability. Gridded observations spanning more than a century show that temperature and precipitation 1901-1970 exhibit low frequency variation (~ 20 year wavelength) without any distinct trend. The interval from the late 1960s to mid 1980s is marked by steep precipitation decline and temperature rise, constituting significant drought. Partial rainfall recovery to values below the pre-1960s norm is found from the mid 1990s onward. Temperature and precipitation are generally anti-correlated throughout the historical record due to cloud cover and surface feedbacks, such that cooler than normal temperature is associated with increased wetness, and warmer than normal temperature is associated with drought (e.g., Martin and Thorncroft, 2014).

Mali's interannual climate variability is influenced by several teleconnections, the most important being the North Atlantic Oscillation (NAO), El Niño–Southern Oscillation (ENSO), Atlantic Niño, and conditions across the Mediterranean Sea (Gaetani et al., 2011; Janicot et al., 2001; Giannini et al., 2003; Rowell, 2003). Multi-decade variability is linked mostly to the Atlantic

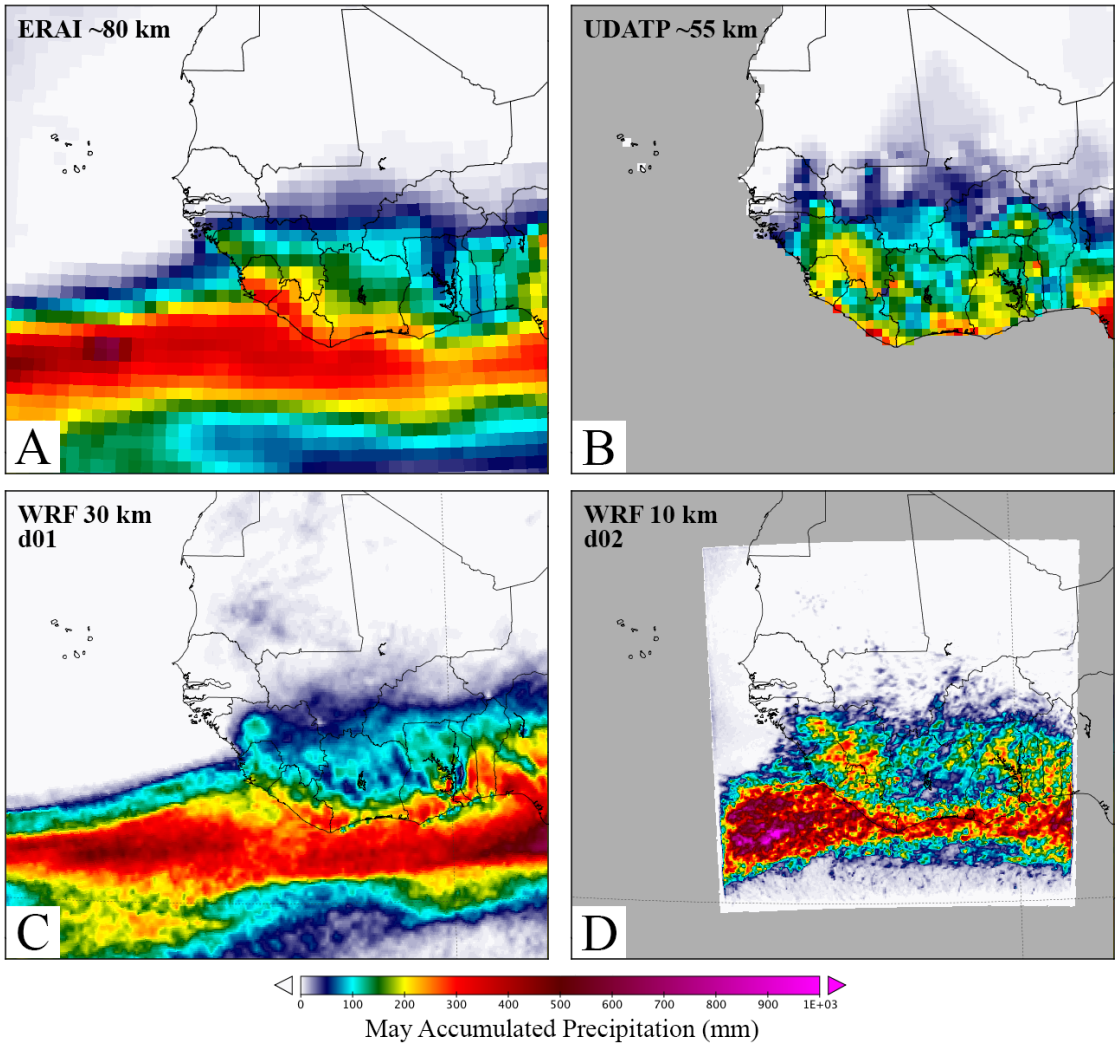

Figure 19. Comparison of May accumulated precipitation for A) ERAI (input reanalysis), B) UDATP gridded observations, C) WRF 30 km outer domain downscale with parameterized convective precipitation, and D) WRF 10 km nested domain with explicit convective precipitation.

Multidecadal Oscillation (AMO) and Pacific Inter-decadal Oscillation (IPO) (Mohino et al., 2010). The transition from AMO-warm to AMO-cold underlies the drought ca. 1960-1990, while re-emergence of AMO-warm drives subsequent rainfall recovery. Failure of rainfall to return to pre-1960s climatology is attributed to increasing tropical ocean surface temperatures from anthropogenic global warming (Mohino et al., 2010).

The importance of the AMO on Mali's climate evolution led us to further characterize the coupling between North Atlantic sea-surface temperatures and atmospheric circulation. A comparison of meteorological maps shows that AMO-warm (1950-1967; also Mali cool/wet) is

associated with NAO-negative type atmospheric patterns (slow winds, shallow Azores-Iceland pressure gradient), whereas AMO-cool (1980-1997; also Mali warm/dry) is associated with NAO-positive (fast winds, steep Azores-Iceland pressure gradient). These opposing climate regimes are coupled to the latitudinal position of the Intertropical Convergence Zone (ITCZ), and strength of the Sahara Low and West African Monsoon (WAM). In all, AMO-warm/NAO-negative is coupled to poleward displacement of the ITCZ, a strong Sahara Low and WAM, and cool/wet conditions across southern Mali, whereas AMO-cool/NAO-positive is coupled to equatorward displacement of the ITCZ, a weak Sahara Low and WAM, and warm/dry conditions across southern Mali.

In a climate system unmodified by humans, the origin of the AMO may be ocean-atmosphere response to volcanism and changes in solar activity (Knudsen et al., 2014). A key line of evidence is that intervals of AMO-cool overlap decisively with periods of high volcanic activity indicated from global aerosol optical depth estimates. Furthermore, major volcanic eruptions are known to impact Northern Hemisphere circulation by inducing NAO-plus (strong winds, steep Azores-Iceland pressure gradient) type atmospheric patterns (Driscoll et al., 2012), which is consistent with our findings above for circulation during AMO-cool. The behavior of the coupled ocean-atmosphere system will likely evolve as greenhouse-gas warming and stratospheric ozone depletion continue to alter boundary conditions.

In relation to the AMO/NAO, we flesh out the role of westerly winds in large-scale circulation across the North Atlantic. We find that SSTs in the subpolar region south of Greenland co-vary with 10-meter wind speed and the pressure difference between Azores and Iceland. Moreover, there is strong correspondence between subpolar SST, wind speed, and precipitation across Mali, where westerly wind speed increases (or declines) as SST and Sahelian rainfall decline (or increase). This is particularly important, because subpolar SSTs south of Greenland are commonly thought to vary by changes in strength of Atlantic Meridional Overturning Circulation (AMOC) in the ocean, but results presented here suggest wind-stress as a driving mechanism. The signal of Sahelian drought and partial recovery after the 1950s is furthermore well represented by changes in mean jetstream winds averaged across the Northern Hemisphere from 30°N-60°N, again emphasizing the fundamental role of atmospheric teleconnections in Mali's climate evolution.

In examination of CMIP5 general circulation model (GCM) output for Mali, we find that temperature and precipitation in historical simulations fail to validate against observations. Most notably, the simulated annual cycle has significant cool temperature bias and precipitation deficit, while annual timeseries lack pattern-match and multi-decade variability. Atmospheric circulation across the North Atlantic is furthermore anomalously strong in CMIP5 due to an unrealistically steep pressure gradient between Azores and Iceland. These shortcomings undermine the fidelity and meaning of CMIP5 future rainfall projections across the western Sahel. We conclude from the above, and from a trial regional climate model simulation, that downscale studies should target reanalysis, and investigate extreme years (e.g., cool/wet or hot/dry) as future climate analogs rather than depend on CMIP5.

In all from this work, we suggest five plausible future climate scenarios for 2030-2050:

- Standard CMIP5 projection of 2 °C warming with slight rainfall decline.

- Annual temperature rise > 1 °C with rainfall remaining at present norm, or increasingly slightly. Generally abundant rainfall results from the ITCZ either maintained or nudged poleward from present climatology by the effect of tropical SST warming concentrated in the North Atlantic. Rainfall delivered with greater intensity due to enhanced convection.

- Annual temperature rise > 1 °C with diminished rainfall or drought. Less rainfall results from the ITCZ nudged southward from present climatology by the effect of tropical SST warming concentrated in the South Atlantic.

- Annual temperature rise > 1 °C with onset of severe drought arising from renewal of high volcanic activity and subsequent development of strong NAO-positive circulation and cool-AMO sea-surface temperature distribution.

- Abrupt climate shift in response to collapse of summer Arctic sea ice, wherein any of the scenarios above could develop within a decade.

References

Bader, J., Latif, M., 2003. The impact of decadal-scale Indian Ocean sea surface temperature anomalies on Sahelian rainfall and the North Atlantic Oscillation. Geophysical Research Letters 30(22): 2169. DOI: 10.1029/2003GL018426.

Biasutti, M., Giannini, A., 2006. Robust Sahel drying in response to late 20th century forcings. Geophysical Research Letters 33, L11706, doi:10.1029/2006GL026067.

Biasutti, M., Sobel, A.H., Camargo, S.J., 2009. The role of the Sahara Low in summertime Sahel rainfall variability and change in the CMIP3 Models. Journal of Climate, 22, 5755–5771, doi: http://dx.doi.org/10.1175/2009JCLI2969.1.

Clark, P.U., Marshall, S.J., Clarke, G.K.C., Hostetler, S.W., Licciardi, J.M., Teller, J.T., 2001. Freshwater forcing of abrupt climate change during the last glaciation. Science, 293(5528), 283-287, doi:10.1126/science.1062517.

Clement, A., Bellomo, K., Murphy, L.N., Cane, M.A., Mauritsen, T., Radel, G., Stevens, B., 2015. The Atlantic Multidecadal Oscillation without a role for ocean circulation. Science 350(6258): 320, DOI: 10.1126/science.aab3980.

Cook, K.H., 1999. Generation of the African Easterly Jet and Its Role in Determining West African Precipitation. J. Climate, 12, 1165–1184. doi:http://dx.doi.org/10.1175/1520-0442(1999)012<1165:GOTAEJ>2.0.CO;2

Driscoll, S., Bozzo, A., Gray, L.J., Robock, A., Stenchikov, G., 2012. Coupled Model Intercomparison Project 5 (CMIP5) simulations of climate following volcanic eruptions. J. Geophys. Res. 117, D17105, doi:10.1029/2012JD017607.

Ebita et al., 2011. The Japanese 55-year Reanalysis JRA-55: An Interim Report. SOLA 7, 149-152.

Enfield, D.B., Mestas-Nunez, A.M., Trimble, P.J., 2001. The Atlantic multidecadal oscillation and its relationship to rainfall and river flows in the continental US. Geophys. Res. Lett. 28, 2077–2080.

Francis, J.A., Vavrus, S.J., 2015. Evidence for a wavier jet stream in response to rapid Arctic warming. Environ. Res. Letters, 10, doi:10.1088/1748-9326/10/1/014005. http://iopscience.iop.org/1748-9326/10/1/014005/article.

Gaetani, M., Pohl, B., Douville, H., Fontaine, B., 2011. West African Monsoon influence on the summer Euro-Atlantic circulation. Geophysical Research Letters, 38, L09705, doi: 10.1029/2011GL047150.

Giannini, A., Saravanan, R., Chang, P., 2003. Oceanic forcing of Sahel rainfall on interannual to interdecadal time scales. Science 302: 1027–1030.

Hartmann, D.L., Wallace, J.M., Limpasuvan, V., Thompson, D.W.J., Holton, J.R., 2000. Can ozone depletion and global warming interact to produce rapid climate change? PNAS 97(4), 1412-1417.

Hoerling, M.P., Hurrell, J.W., Eischeid, J., 2006. Detection and attribution of 20th century Northern and Southern African monsoon change. Journal of Climate 19, 3989-4008.

Janicot S., Trzaska, S., Poccard, I., 2001. Summer Sahel-ENSO teleconnection and decadal time scale SST variations. Climate Dynamics 18: 303-320.

Kalnay, E., et al., 1996. The NCEP/NCAR 40-year reanalysis project. Bull. Am. Meteorol. Soc. 77: 437-471.

Knudsen, M.F., et al., 2014. Evidence for external forcing of the Atlantic Multidecadal Oscillation since termination of the Little Ice Age. Nat. Commun. 5:3323, doi: 10.1038/ncomms4323.

Lamb, P.J., 1978. Large-scale tropical Atlantic surface circulation patterns associated with subsaharan weather anomalies. Tellus 30: 240-251.

Lee, S., Fieldstein, S.B., 2013. Detecting ozone-and greenhouse gas-driven wind trends with observational data, Science 339(6119), 563-567, DOI: 10.1126/science.1225154.
Martin, E.R., Thorncroft, C.D., 2014. The impact of the AMO on the West African monsoon annual cycle, Q. J. R. Meteorol. Soc. 140: 31-46.
Mohino, E., Janicot, S., Bader, J., 2010. Sahel rainfall and decadal to multi-decadal sea surface temperature variability. Climate Dynamics, doi: 10.1007/s00382-010-0867-2.
Perlwitz et al., 2008. Impact of stratospheric ozone hole recovery on Antarctic climate. Geophysical Research Letters, 35, 8, DOI: 10.1029/2008GL033317.
Polvani, L.M., et al., 2011. Stratospheric Ozone Depletion: The Main Driver of Twentieth-Century Atmospheric Circulation Changes in the Southern Hemisphere. J. Climate 24, 795-812.
Schneider, U. et al., 2013. GPCC's new land surface precipitation climatology based on quality-controlled in situ data and its role in quantifying the global water cycle. Theoretical and Applied Climatology http://dx.doi.org/10.1007/s00704-013-0860-x.
Shindell, D.T., Schmidt, G.A., Mann, M.E., Faluvegi, G., 2004. Dynamic winter climate response to large tropical volcanic eruptions since 1600. Journal of Geophysical Research 109, D05104, doi:10.1029/2003JD004151.
Skamarock, W. C., et al., 2008. A description of the advanced research WRF version 3, NCAR, Tech. Note, Mesoscale and Microscale Meteorology Division. National Center for Atmospheric Research, Boulder, Colorado, USA.
Sultan, B., Janicot, S., 2003. The West African Monsoon Dynamics. Part II: The "Preonset" and "Onset" of the Summer Monsoon. J. Climate 16, 3407-3427. doi: http://dx.doi.org/10.1175/1520-0442(2003)016<3407:TWAMDP>2.0.CO;2
Willmott, C.J., Matsuura, K., 2001. Terrestrial Air Temperature and Precipitation: Monthly and Annual Time Series (1950 - 1999), http://climate.geog.udel.edu/~climate/html_pages/README.ghcn_ts2.html.
Wunsch, C., 2006. Abrupt climate change: An alternative view. Quaternary Research 64, 191-203.
Liang, X-Z, Kunkel, K.E., Meehl, G.A., Jones, R.G., Wang, J.X.L, 2008. Regional climate models downscaling analysis of general circulation models present climate biases propagation into future change projections. Geophysical Research Letters 35, L08709, doi:10.1029/2007GL032849.
Zeng, N., 2003. Drought in the Sahel. Science 302, 999-1000.